ISSN: 2469-9062 (print), 2467-9240(e)

Journal of Institute of Science and Technology, 2015, ***20(1):*** *20-27, © IOST, Tribhuvan University*

Dynamics Ionospheric Plasma Bubbles Measured by Optical Imaging System

Narayan P. Chapagain
Department of Physics, Patan M. Campus
Tribhuvan University, Kathmandu, Nepal
Email:- npchapagain@gmail.com

ABSTRACT

Deep plasma depletions during the nighttime period in the equatorial ionosphere (referred to as equatorial plasma bubbles –EPBs) can significantly affect communications and navigation systems. In this study, we present the image measurements of plasma bubble from Christmas Island (2.1°N, 157.4°W, dip latitude 2.8°N) in the central Pacific Ocean. These observations were made during September-October 1995 using a Utah State University (USU) CCD imaging system measured at ~280 km altitude. Well-defined magnetic field-aligned plasma depletions were observed for 18 nights, including strong post-midnight fossilized structures, enabling detailed measurements of their morphology and dynamics. We also estimate zonal velocity of the plasma bubbles from available images. The zonal drift velocity of the EPBs is a very important parameter for the understanding and modeling of the electrodynamics of the equatorial ionosphere and for the predictions of ionospheric irregularities. The eastward zonal drift velocities were around 90-100 m/s prior to local midnight, and decreases during the post-midnight period that persisted until dawn.

Keywords: Ionosphere, irregularities, plasma depletion, optical imaging, equatorial plasma bubble.

INTRODUCTION

The ionosphere is the ionized region of the upper atmosphere extending from ~50 km to beyond 1000 km from the surface of the Earth. This region contains significant numbers of free electrons and positive ions and also some negative ions. The electron concentration may amount to only about one percentage of the neutral concentration. However, the presence of these electrons has a profound effect on the properties and behaviour of the medium. The vertical structure of the ionosphere has been divided into three layers according to ion constituent and associated chemistry (Kelley 1989). These distinct layers are formed due to (i) the solar spectrum deposits its energy at various heights depending on the absorption characteristics of the atmospheric constituents, (ii) the physics or recombination process that depends on the atmospheric density, and (iii) the composition of the atmosphere changes with altitudes. The main layers of the ionosphere are D-region (~50-90 km altitude), E-region (~90-150 km altitude), and F-region (150-500 km altitude) (Kelley 1989). The layers are generally characterized by density maxima at a certain altitude. The D-layers is mostly responsible for the refection of low frequency radio waves propagation from earth during the daytime. While during the nighttime the D-layer vanishes and E-layer becomes very weak and consequently, the F-layer is primarily responsible for the reflection and propagation of the radio waves in the Earth's atmosphere.

The Earth's ionosphere often shows the occurrence of highly irregular plasma density and the fluctuations of velocity with a large range of scale sizes and amplitudes almost at all altitudes throughout the latitude and longitude sectors. Such plasma irregularities at F-region ionosphere are predominantly a nighttime phenomenon and this is a region of greatest interest to space community because of the complex dynamical phenomena and instability occurrence in this region. This post-sunset phenomenon is commonly referred to as plasma irregularity or plasma depletion or plasma bubble. These plasma irregularities are generally magnetic field aligned, which have zonal widths of typically a few tens of kilometres and extend along the magnetic field lines for hundreds to thousands of kilometres depending on the peak altitude of the irregularity (bubble) development (Sobral *et al.* 2002), while their vertical heights range from a few tens of kilometres to several hundred kilometres.

When radio signals propagate through these irregularity regions, they cause distortion in amplitude and phase of radio waves leading to the loss of signal strength directly affecting the communication and navigations systems and hence all sector of public life. The generation of these irregularities is one of the most spectacular manifestations of space weather in the Earth's ionosphere. Understanding the day-to-day variability of these irregularities has become a highly active area of

research, particularly, in the aeronomy community but a complete understanding of this phenomenon is yet to be achieved and much work remains to be done before we have a complete understanding of this phenomenon.

Ionospheric irregularities were first reported by using via High-Frequency (HF) radio ionospheric sounding experiments about seven decades ago. Berkner and Wells (1934) described well-known accounts of ionosonde reflections above the nighttime F peaks. Booker and Wells (1938) published night time ionograms with virtual height traces that were mysteriously spread in altitude. The bottomside profiles of the plasma were also found to be disturbed after sunset, which affected radio wave propagation near the critical frequency. The critical frequency is the highest magnitude of frequency above which the waves can penetrate the ionosphere, while below this frequency, waves are reflected back from the ionosphere. Such types of ionospheric disturbance, is now known as the process that causes large-scale plasma depletions. As the plasma depletions advect upwards from the bottomside to the topside ionosphere, they generate a broad spectrum of disturbances that can be detected by digital ionosondes and ionospheric radars and result in spectacular airglow images. Haerendel (1973) published a theory for bubbles where he applied the concept of flux tube integrated variables. Hanson and Sanatoni (1973) used the satellite observations and reported density bite-outs of over three orders of magnitude deep in the bottomside F-region. Woodman and LaHoz (1976) used radar observations from Jicamarca, Peru, and reported plume-like structures extending to high altitudes. In addition to the ionosonde and radar observations (Fejer & Kelley 1980, Chapagain *et al.* 2009), the plasma irregularities have been detected by satellite (*M*cClure *et al.* 1977), rockets (Kelley *et al.* 1982) as well as other ground-based optical instruments (Weber *et al.* 1978, Mendillo & Baumgardner 1982, Taylor *et al.* 1997).

The plasma bubbles development is most effective at the magnetic equator in the post-sunset time period, although occasionally post-midnight and pre-sunrise events have also been observed. These bubbles sometimes reach more than 20º magnetic latitude from the generation region at the magnetic equator (Kelley *et al.* 2002, Makela & Kelley 2003) This is due to the large conductivity along the magnetic field lines, allowing the perturbed electric fields to efficiently map poleward where they can affect the local ionosphere. For example, the irregularities developed in the equatorial region say above the south India (magnetic equatorial region) can propagate poleward above the Nepal where magnetic latitude is around 18º. Hence the study of these irregularities also becomes important in Asian territories including Nepal.

The bubbles extending poleward of the equator allow for ground-based imaging techniques to capture two-dimensional spatial information on the depletions. Several previous studies have employed all-sky imagers pointed to the zenith to make observations of depleted regions of scale size in order of a kilometre to several kilometre associated with irregularities (Mendillo & Baumgardner 1982, Taylor *et al.* 1997, Makela 2006, Chapagain *et al.* 2011). The advantage of imaging over other techniques such as coherent radar observations, VHF scintillation etc. for studying these irregularities is that imaging reveals the two-dimensional structure of these depleted regions rather than their properties along a single viewing direction.

In this study, we present the optical observations near magnetic equator from Christmas Island in the Central Pacific ocean to examine the signature of ionospheric plasma bubbles as observed by optical imaging technique. We also estimate the zonal drift velocity of the plasma bubbles to probe the distance travelled by the bubbles once it originates at a place.

MATERIALS AND METHODS

As the airglow is faint, we cannot see it readily because the strongest airglow emission lies in the infrared region, which is beyond the range of human's eye sensitivity (Wayne 1991). However, we can use sensitive optical equipment, such as photometers and CCD cameras, to observe airglow emissions during the nighttime period. As atmospheric disturbances, such as internal gravity waves, pass through the airglow layers, they cause perturbations in the temperature and density of the relevant constituents, which in turn, produce intensity fluctuations of the airglow. These intensity variations are used to study the disturbances in the upper atmosphere, including the ionospheric plasma irregularities.

The ionospheric plasma bubble is measured by observing the OI (630.0 nm) airglow intensity depletion. However, the volume emission rate of 630.0 nm O(^{1}D) decreases at higher altitudes as molecular oxygen density exponentially decays with height. As a result, the higher minimum F-layer height required for bubble formation leads to low airglow intensities. Thus, it is unlikely that the development of bubbles after sunset will be observed through 630.0 nm airglow photometry near the magnetic equator. When the post-sunset ionosphere decreased in virtual height to less than ~275 km, airglow intensities increases and hence the fully developed depletions may became visible as dark bands in the ambient airglow. On the other hand, when the virtual height at the magnetic equator is above ~275 km for the entire night, the airglow depletion will not be visible, even though bubbles

and scintillations might have occurred (Mendillo & Baumgardner 1982).

The development of highly sensitive CCD cameras has proven to be an ideal instrument for the imaging of nighttime airglow in the sky and for the study the upper atmospheric phenomenon. The imaging system consists of an all-sky or fish-eye (180˚FOV) lens system, a computer-controlled filter wheel, and a CCD camera head fitted with a 1024×1024 pixel back-illuminated bare CCD (quantum efficiency ~80% at visible and 50% at NIR wavelengths). Taylor and Hill (1991) were able to obtain high-quality images of wave structure using a CCD camera. These cameras were first used for narrow field of view (FOV) measurements. They further developed a fish-eye (180˚ FOV) lens to image airglow emissions. Taylor and Garcia (1995) published the first results using this method for the airglow measurements. Since then, many studies have been carried out using this technique (Taylor *et al.* 1997, Santana *et al.* 2001, Makela & Kelley 2003, Mukherjee 2003, Martinis *et al.* 2003, Pautet *et al.* 2009, Chapagain *et al.* 2011, Chapagain *et al*. 2013).

OBSERVATION AND DATA ANALYSIS

The CCD airglow imager from Utah State University (USU), USA, was deployed at Christmas Island, Republic of Kiritimati (2.1°N, 157.4°W, dip latitude 2.8°N) for exploratory optical measurements of ionospheric plasma bubbles in the central Pacific sector. The measurements were made for 18 nights from 14 September to 03 October 1995. The images were recorded on time intervals of approximately 5 and 11 minutes of sequence of observations. But this data were not analysed before in detail. In this paper we have analysed these data to study the occurrence, spatial characteristics, and dynamics of the ionospheric plasma bubbles at equatorial latitudes.

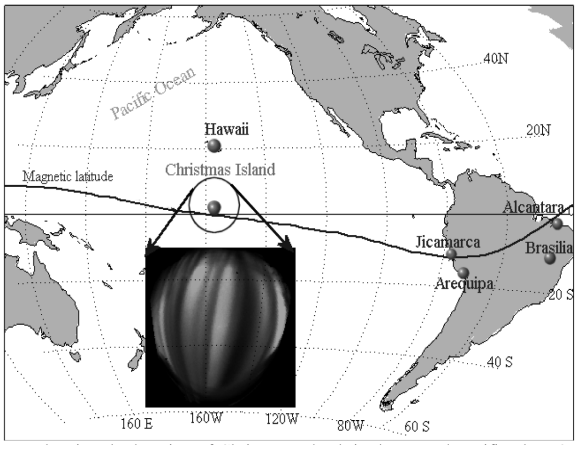

Fig. 1. Map showing the location of Christmas Island, in the central Pacific, the FOV covered by the all-sky imager (circle), and an example of OI (630.0 nm) airglow image. The solid line represents the magnetic equator.

Fig. 1 is a map of the Pacific region that shows the Chirstmas Island at about 2000 km due south of Hawaii, USA. The open circle centred over Christmas Island represents the geographic field of view (FOV) covered by the all-sky imager of about 1500 km diameter for F-region measurements assuming a reference altitude of airglow emissions at 280 km. The enlarged airglow image below illustrates the orientation and typical structure of plasma bubble recorded during the campaign. The solid curve line show the magnetic equator.

RESULTS

Equatorial Plasma Bubbles (EPBs)

The occurrence of the nighttime plasma irregularities in the equatorial F-region ionosphere is commonly referred to as equatorial plasma bubbles (EPBs). The wide spectral distribution of EPBs are known to cause interference with satellite-to-ground-based telecommunication channels, and the degradation of navigation and Global Position systems (GPS) due to the random fluctuations of the amplitude and phase of the radio waves as they pass thorough these irregularity regions (Basu *et al.* 1999).

The ionospheric irregularities have broad range of scale sizes over several orders of magnitude from tens of centimetres to hundreds of kilometres. They extend from the F-region (~200 km) up to ~2000 km altitudes within the dip latitudes of about ±20° and are driven by a number of wave generation processes (Chapagain *et al.* 2011). Due to the high parallel conductivity and mobility in the ionosphere, the signature of irregularities can be observed in all latitudes between low and mid-latitude (~20°) regions. The spread F occurrences in the equatorial F-region can be particularly severe, although they can appear at all latitudes. However, their occurrences depend on the season, solar cycle, latitude, and longitude.

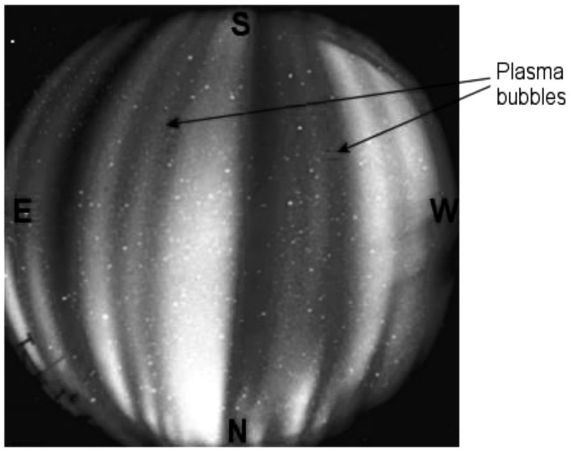

Fig. 2. Example of processed image recorded by the USU optical imager from Christmas Island.

Fig. 2 shows an example of an OI (630.0 nm) airglow image measured by the USU all-sky CCD camera on September 28, 1995 from Christmas Island obtained from processing the raw image taken by CCD camera. For the image processing, we use the software developed by the Centre for Atmosphere and Space Sciences (CASS), from Department of Physics, Utah State University, USA. A fully developed night time irregularity is characterized by plasma bubbles that are the region of the deep plasma depletion as shown by the dark bands on the image (Fig. 2). The plasma density inside the bubbles can be up to three orders of magnitude lower than that of its surroundings. During the development phase of the plasma bubbles, they are known to drift upward and eastward. When the irregularities onset ends, generally during the post-midnight period, the upward drifts ceases and the fully developed bubbles, move together with the ambient plasma drift as "fossilized" structures in eastward.

EPB Zonal Velocity

The zonal velocities of EPB as a function of local solar time (LST) were measured on 18 near-consecutive nights. First we processed the raw images using the software developed by USU, USA and these images were used to determine an average drift velocity for each depletion structure. To calculate the bubble velocity, the displacement of an individual structure was measured from two consecutive images. The speeds were then estimated by dividing the average distance between the structures by the corresponding time interval. The drift velocities are usually calculated from bubbles as they move through the zenith sky. However, these data were often need to be supplemented by measurements of bubbles closer to the edges of the camera's FOV adjusting to the same LST.

Fig. 3 shows the derived zonal velocity of several consecutive EPBs as a function of LST during the night of 28-29 September 1995. The OI image at 23:51 LST shows an example of bubble structures (numbered 1-7), but several other bubbles were also measured during the same night. The drift velocity of each bubble overlaps very well. The average velocity indicated by the bold line peaked at ~115 m/s around 23:00 LST and then decreases over the next ~2 hours down to ~60 m/s, and thereafter nearly remained about to constant until at dawn ~5:00 LST.

Using the above procedure, Fig. 4 shows the average EPB zonal drift velocities as a function of LST for 16 nights of the campaign. Due to limitations in the camera operation caused by moonlight, the measurements were restricted to evening time during the first part of the campaign and the post-midnight during the latter part on the campaign. However, it is clear from the Fig. 4 that good measurements were obtained during most of the campaign period. The gaps in the drift velocity data on 15-16, 18-19, 20-21 and 24-25 September 1995 were due to clouds, while on 21-22, 29-30 September and 30 September-1 October, they were caused by strong fading of the bubbles. The vertical bars on each plot represent one standard deviation in the measurement uncertainty at that time.

To examine the influence of the magnetic activity on zonal drift velocity of EPBs, we checked the average values of three hourly geomagnetic indexes <Kp> over a nine-hour period (13:30-22:30 LST) and are given in each plot. We classify the observation days in such a way that the days are geomagnetically quiet if the average

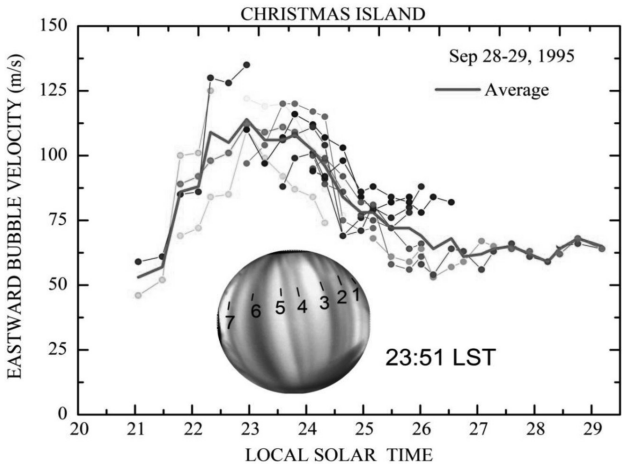

Fig. 3. EPBs drift velocities for several consecutive bubbles on September 28-29. Examples of bubble numbers (1, 2, 3, 4, 5, etc.) are also shown in the OI image at 23:51 LST. The bold line represents the averaged velocity of all bubbles.

values of K_p index are less than 3, otherwise, the days are said to be geomagnetically disturbed. In this calculation, the interval includes six hours prior to local sunset during which EPB onset may be influenced by geomagnetic storms. However, the geomagnetic activity was quiet with minor activity (< 3) except in 15 and 28 September 1995, when $<K_p>$ was slightly larger than 3 and hence no significant difference in EPB activity was evident. This result was actually a expected one since geomagnetic storms during solar minimum condition are less likely to affect, are known not to significantly affect zonal drift velocities. However, the storms prior to sunset may still inhibit the onset of ESF (Fejer *et al*. 2005).

Fig. 4 reveals a significant night-to-night variability in the derived EPBs drift velocities. On several nights, they generally increase in early evening hours, peaking around 22:00-23:00 LST (velocities >100 m/s). The

velocities then decrease to a minimum around local solar midnight and then increase slightly in magnitude in the early morning hours. On the other hand, in some nights (e.g., 22-23 September) exhibit very little change in the magnitude of the velocity, which remains relatively high throughout the night. Fig. 4 also shows small eastward velocity of ~7 m/s, and westward velocity of ~20 m/s in the early evening hours on September 26-27, and September 24-25, respectively.

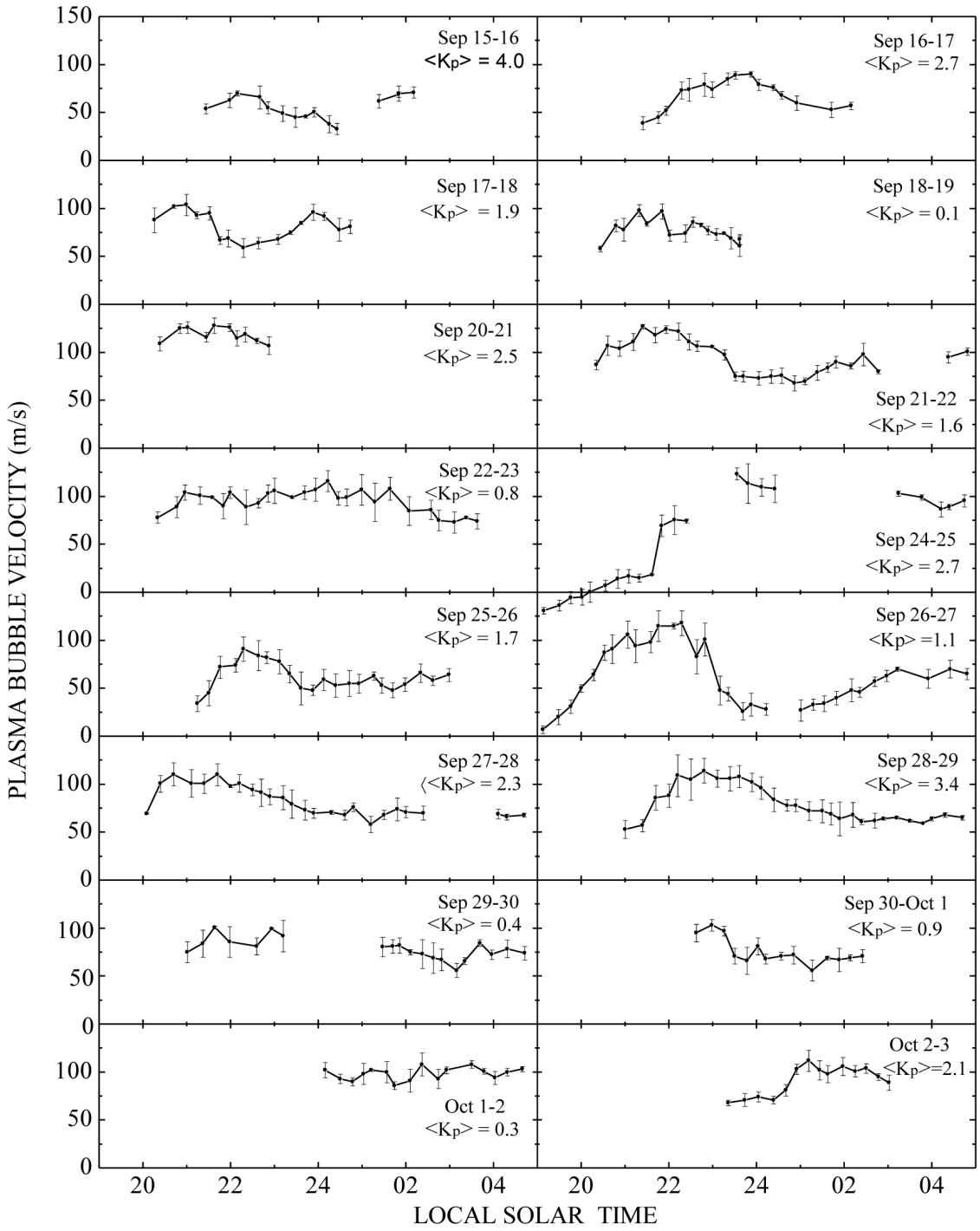

Fig. 4. The average EPBs drift velocities calculated from two successive images for time binned at ~16 minutes during 16 nights, assuming a reference altitude of airglow emissions at 280 km. In the plot K_p index represents average geomagnetic activity during nine-hour period.

DISCUSSION

The occurrence and severity of irregularity event depends on the condition of the local equatorial ionosphere, as well as that of the plasma in electrical contact with it (namely, the off-equatorial E-region) through coupling within the appropriate magnetic flux tube. Convective plumes of turbulent plasma that develop during strong ESF events rising to higher altitudes can degrade communications system and can last for several hours as the plumes (bubbles) drift as the fossilized bubbles with the background plasma. Consequently, further study on the development and propagation of the plasma bubbles during the night-time has become very important for space weather predictions. Additionally, the knowledge of space and time variations of the ionospheric zonal and vertical drifts velocities in the equatorial region is of fundamental importance for the understanding of the low-latitude ionospheric climatology (Fejer *et al.* 1991). The study of these drifts also helps us to better understand the local mechanisms of coupling processes of the ionosphere-thermosphere (I-T) system under geomagnetically quiet conditions, including global mechanisms of the equatorial ionosphere coupling with magnetosphere, interplanetary medium and high-latitude I-T system under geomagnetically disturbed conditions.

The depletions observed from Christmas Island are clearly similar to OI (630.0 nm) thermospheric observations from other sites at equatorial regions. Their magnetic meridian alignment, sharp east-west gradients in the airglow structure and spacing of the dark bands strongly suggest that they are the airglow signature of the medium scale field-aligned EPBs generated by the Rayleigh-Taylor instability. Studies of equatorial ionospheric irregularities using Atmospheric Explorer E (AE-E) plasma density measurements reported that such irregularities have the form of sharp quasi-periodic depletions (Tsunoda *et al.* 1982, Hysell & Kelley 1997). Abalde *et al.* (2001) presented the fine structure of the quasi field-aligned ionospheric EPBs using the OI777.4 nm emission image measurements. Since the Christmas Island observations were made from close to the dip equator, the results only show the airglow structure of the bottomside F region modulations in the plasma depletions (altitude ranges of ~ 200-400 km). Therefore, these data cannot demonstrate that these F region EPBs structures penetrated to the topside ionosphere, though they likely did. Particularly in the early evening, some bubbles structures may only have been bottomside modulations, yet to grow into topside bubbles. For most of the nights, the depletions developed in the FOV of the camera during early evening and then drifted eastward. They are seen close to 19:30 LST (1 hour after ground level local sunset) to 04:00 LST (09:30 hour after local sunset). Thus, these early evening plasma depletions and possible EPBs have their initial development near Christmas Island longitude. Later in the evening airglow signatures of plasma depletions forming at other longitudes drifted into the FOV as fossilized depletions just as observed by Makela *et al.* (2004). The airglow signatures of the fossilized structures sometimes will remain until local sunrise when the sun re-ionizes the ionosphere.

CONCLUSIONS

In this study, night-time EPBs observations from Christmas Island located in the central Pacific ocean using all-sky images of the thermospheric OI (630.0 nm) airglow emissions have been reported. The large scales EPBs aligned along the Earth's magnetic field are observed on every night of the campaign. The EPBs mostly developed early evening hours during 19:30–20:00 LST and their active growth region was close to the west edge of camera's FOV suggesting that they were seeded to the west of Christmas Island.

The EPBs developed in the early evening propagate eastward as fossilized structures that persisted till the dawn during the most of the night of the observations. The EPBs drift velocities exhibited significantly day-to-day variations in their magnitudes which increased as night progress and becomes peaked around 90–100 m/s at ~23:00 LST at approximately 2 hours after local sunset. The bubbles drift velocities remains at a nearly constant at the value of ~80 m/s during the post-midnight period until dawn. The further study of morphology and dynamics of EPBs from different latitude and longitude sectors is important to investigate the onset as well as growth of EPBs. Moreover, we are also planning to investigate the ionospheric conditions over Nepal by using the satellite data observations. We are also working to deploy an optical imaging system at Nagarkot, Solar Observatory in collaboration with Utah Valley University, USA so that we can study the dynamics of ionospheric irregularities over Kathmandu.

ACKNOWLEDGEMENTS

I would like to thank Prof. Mike Taylor, Centre for Atmosphere and Space Sciences, Utah State University, Logan, UT, USA for providing the data for this study.

REFRENCES

Abalde, J.R., Fagundes, P.R., Bittencourt, J.A. and Sahai Y. 2001. Observations of equatorial F region plasma bubbles using simultaneous OI 777.4 nm and OI 630.0 nm imaging: New results, *J. Geophys. Res.* **106**(A12): 30331-30336, doi:10.1029/2001JA001115.

Basu, S., Groves, K.M., Quinn J.M., and Doherty P. 1999. A comparison of TEC fluctuation and scintillations at Ascension Island, *J. Atmos. Sol.-Terr. Phys.* **61:** 1219- 1226.

Berkner, L.V., and Wells, H.W. 1934. F-region ionosphere – Investigation at low latitudes. *Terres. Magn.* **39:** 215.

Booker, H.G. and Wells, H.W. 1938. Scattering of radio waves by the F-region of the ionosphere. *J. Geophys. Res.* **43**: 249-256.

Chapagain, N.P., Fejer, B.G., and Chau, J.L. 2009. Climatology of postsunset equatorial spread F over Jicamarca. *J. Geophys. Res.* **114:** A07307, doi:10.1029/2008JA013911.

Chapagain**,** N. P., Taylor, M.J., and Eccles J.V. 2011. Airglow observations and modeling of F region depletion zonal velocities over Christmas Island. *J. Geophys. Res.* **116:** A02301, doi:10.1029/2010JA015958.

Chapagain, N.P., Fisher, D.J., Meriwether J.W., Chau J.L. and Makela J.J. 2013. Comparison of zonal neutral winds with equatorial plasma bubble and plasma drift velocities. *J. Geophys. Res. Space Physics* **118:** doi:10.1002/jgra.50238.

Fejer, B.G., and Kelley, M.C. 1980. Ionospheric irregularities. *Rev. Geophys.* **18:** 401-454.

Fejer, B.G., de Paula, E.R., Gonzalez, S.A., and Woodman, R.F. 1991. Average vertical and zonal F region plasma drifts over Jicamarca. *J. Geophys. Res.* **96**(A8): 13901-13906, doi:10.1029/91JA01171.

Fejer, B.G., Souza, J.R., Santos, A.S., and Cost Pereira A.E. 2005. Climatology of F region zonal plasma drifts over Jicamarca. *J. Geophys. Res.* **110:** A12310, doi:10.1029/2005JA011324.

Haerendel, G. E. 1973. Theory of equatorial spread F, Report. *Max Planck Institut fur Extraterre. Phys.,*Garching, Germany.

Hanson, W. B., and Sanatani, S. 1973. Large Ni gradients below the equatorial F peak. *J. Geophys. Res.* **78:** 1167-1172.

Hysell, D.L., and Kelley, M.C. 1997, Decaying equatorial F region plasma depletions. *J. Geophys. Res.* **102:** (A9), 20,007–20,017, doi:10.1029/97JA01725.

Kelley, M.C., Pfaff, R., Baker, K.D., Ulwick, J.C., Livingston R., Rino, C., and Tsunoda R. 1982. Simultaneous rocket probe and radar measurements of equatorial spread F – transitional and short wavelength results, *J. Geophys. Res.* **87:** 1575.

Kelley, M.C. 1989. The Earth's Ionosphere: Plasma physics and electrodynamics. **43:** *Academic Press,* San Diego, California.

Kelley, M.C., J.J. Makela, B.M. Ledvina, and P.M. Kintner 2002. Observations of equatorial spread F from Haleakala, Hawaii. *Geophys.Res. Lett.* **29:** doi:10.1029/2002GL015509.

Makela, J.J. 2006. A review of imaging low-latitude ionospheric irregularity processes, *J. Atmos. Sol.-Terr. Phys.* **68:** (13):1441–1458.

Makela, J. J., and M. C. Kelley 2003. Field-aligned 777.4 nm composite airglow images of equatorial plasma depletions, *Geophys. Res. Lett.* **30:** (8).

Makela, J.J., Ledvina B.M., Kelley M.C. and Kintner, P.M. 2004. Analysis of the seasonal variations of equatorial plasma bubble occurrence observed from Haleakala, Hawaii. *Ann. Geophys* **22**: 3109-3121, doi:10.5194/angeo-22-3109-2004.

Martinis, C., Eccles, J.V., Baumgardner, J., Manzano J. and Mendillo, M. 2003. Latitude dependence of zonal plasma drifts obtained from dual site airglow observations. *J. Geophys. Res.* **108**(A3): 1129, doi:10.1029/2002JA009462.

McClure, J.P., Hanson, W.B., and Hoffman, J.H. 1977. Plasma bubbles and irregularities in the equatorial ionosphere. *J. Geophys. Res.* **8:** 2650.

Mendillo, M. and Baumgardner, J. 1982. Airglow characteristics of equatorial plasma depletions. J. Geophys. Res. **87**(A9): 7641-7652, doi:10.1029/JA087iA09p07641.

Mukherjee, G. K. 2003. Studies of equatorial F-region depletions and dynamics using multiple wavelength nightglow imaging. *J. Atmos. Terr. Phys.* **65:** 379-390.

Pautet, P.D., Taylor M.J., Chapagain, N.P., Takahashi, H., Medeiros, A.F., Sao Sabbas, F.T. and. Fritts, D.C. 2009. Simultaneous observations of equatorial F region plasma depletions over Brazil during the Spread F Experiment (SpreadFEx). *Ann. Geophys.* **27:** 2371-2381, doi:10.5194/angeo-27-2371-

Santana, D. C., Sobral, J.H.A , Takahashi H., and Taylor, M.J. 2001. Optical studies of the ionospheric irregularities over the Brazilian region by nocturnal images of the OI (630.0 nm) emission. *Adv. Space Res.* **27:** 6, 1207-1212(6).

Sobral, J.H.A., Abdu, M.A., Takahashi, H., Taylor, M.J., de Paula, E.R., Zamlutti,. C.J., de Aquino, M.G and Borba, G.L. 2002. Ionospheric plasma bubble climatology over Brazil based on 22 years (1977-1998) of 630 nm airglow observations, *J. Atmos. Terr. Phys.* **64:** 1517– 1524.

Taylor, M.J., and Hill M.J. 1991. Near-infrared imaging of hydroxyl wave structure over an ocean site at low latitudes. *J. Geophys. Res.* **18:** 1333-1336.

Taylor, M.J. and Garcia, F.J. 1995. A two-dimensional spectral analysis of short period gravity waves imaged in the OI (557.7 nm) and nearinfrared OH nightglow emissions over Arecibo, Puerto Rico. *Geophys. Res. Lett.* **22:** 2473-2476, doi:10.1029/95GL02491.

Taylor, M. J., Eccles J.V., LaBelle, J., and Sobral, J.H.A. 1997. High resolution OI (630 nm) image measurements of F region depletion drifts during the Guára campaign. *Geophys. Res. Lett.* **24**: 1699-1702, doi:10.1029/97GL01207.

Tsunoda, R.T., Livingston R.C., McClure, J.P. and Hanson W.B. 1982. Equatorial plasma bubbles: Vertically elongated wedges from bottomside F layer. *J. Geophys. Res.* **87:** (A11), 9171-9180, doi:10.1029/ JA087iA11p09171.

Wayne, R.P. 1991. Chemistry of atmospheres: an introduction the chemistry of atmospheres of earth, the planets, and their satellites. *Oxford University Press*, New York.

Weber, E.J., Buchau, J., Eatther, R.H. and Mende S.B.1978. Northsouth aligned equatorial airglow depletions. *J. Geophys. Res.* **83**(A2): 712-716, doi:10.1029/JA083iA02p00712.

Woodman, R.F., and LaHoz C. 1976. Radar observations of F-region equatorial irregularities. *J. Geophys. Res.* **81:** 5447-5466.